STRAIN/DAMAGE IN CRYSTALLINE MATERIALS BOMBARDED BY MeV IONS: RECRYSTALLIZATION OF GaAs BY HIGH-DOSE IRRADIATION

C. R. WIE, T. VREELAND, JR., AND T. A. TOMBRELLO
Divisions of Physics, Astronomy, and Mathematics and Engineering and Applied Science, California Institute of Technology, Pasadena, California 91125

ABSTRACT

MeV ion irradiation effects on semiconductor crystals, GaAs(100) and Si (111) and on an insulating crystal CaF_2 (111) have been studied by the x-ray rocking curve technique using a double crystal x-ray diffractometer. The results on GaAs are particularly interesting. The strain developed by ion irradiation in the surface layers of GaAs (100) saturates to a certain level after a high dose irradiation (typically $10^{15}/cm^2$), resulting in a uniform lattice spacing about 0.4% larger than the original spacing of the lattice planes parallel to the surface. The layer of uniform strain corresponds in depth to the region where electronic energy loss is dominant over nuclear collision energy loss. The saturated strain level is the same for both p-type and n-type GaAs. In the early stages of irradiation, the strain induced in the surface is shown to be proportional to the nuclear stopping power at the surface and is independent of electronic stopping power. The strain saturation phenomenon in GaAs is discussed in terms of point defect saturation in the surface layer.

An isochronal (15 min.) annealing was done on the Cr-doped GaAs at temperatures between 200° C and 700° C. The intensity in the diffraction peak from the surface strained layer jumps at 200° C $< T \leq 300^{\circ}$ C. The strain decreases gradually with temperature, approaching zero at $T \leq 500^{\circ}$ C.

The strain saturation phenomenon does not occur in the irradiated Si. The strain induced in Si is generally very low (less than 0.06%) and is interpreted to be mostly in the layers adjacent to the maximum nuclear stopping region, with zero strain in the surface layer. The data on CaF_2 have been analysed with a kinematical x-ray diffraction theory to get quantitative strain and damage depth profiles for several different doses.

INTRODUCTION

Sadana and coworkers observed that GaAs amorphized by MeV ion irradiation at liquid nitrogen temperature could be reconverted to a single crystal by a subsequent MeV ion irradiation at room temperature [1]. The following experiments show that higher substrate temperature and dense electronic ionization around the path of a bombarding MeV ion can be effective in the suppression of amorphization and in amorphous-to-crystalline reconversion. In an x-ray rocking curve study, a GaAs crystal implanted at room temperature with 300 keV Si ions (where the energy loss process is mainly due to nuclear cascade collisions with comparable energy to this nuclear stopping deposited into the target electronic system only near the surface) gives a small diffraction signal for a $1.2 \times 10^{15}/cm^2$ beam dose [2]. A 220 keV ion implantation at room temperature produces an amorphous layer in GaAs at a beam dose of $10^{13}/cm^2$, whereas the implantation performed at 150° C does not produce an amorphous region at a $10^{15}/cm^2$ dose [3].

Hodgson and coworkers used a pulsed 200 keV proton beam to anneal Si amorphized by 100 keV As ion implantation [4]. Even though the 200 keV proton

beam loses most of its energy into the target electronic system, there is a phenomenological difference between the typical pulsed beam annealing and the keV ion implantation or the MeV ion bombardment. In the pulsed beam annealing, the typical beam current density is 10^{20}-10^{21} ions/cm^2 sec for a proton beam and 10^{21}-10^{22} electrons/cm^2 sec for a pulsed electron beam, so that the cylindrical regions of dense ionization around the particle path heavily overlap instantaneously, and the irradiation region becomes laterally uniform, so the irradiation effect results in the melting of the target from thermal heating. In the MeV ion irradiation, however, the typical particle current density is 10^{11} to 10^{12} ions/cm^2 sec so that the cylindrical ionization regions around each ion path do not overlap appreciably within the relaxation time of the ionized electrons.

MeV ions leave damage tracks [5] in and cause enhanced sputtering from the surface of insulators and some compound semiconductors [6]. The cylindrical damage track structure is ascribed to processes following the dense ionization around the ion path in the target [7]. Elemental semiconductors do not show enhanced erosion by electronic ionization/excitation from MeV ion bombardment [8]. The electronic ionization/excitation effect on the solid surfaces induced by MeV ion bombardment is used for surface modification [9], interfacial changes for the enhancement of thin film adhesion, and for the modification of electrical contact properties [10]. We used a CaF_2 single crystal, a track forming material, to study the strain and damage in the surface layers induced by MeV ions [11].

Among the III-V compound semiconductors, simple defects are essentially immobile near room temperature in GaAs and well above room temperature in GaP; however, the primary defects in GaSb, InSb, and InAs and those in elemental semiconductors, Si and Ge, are all mobile below 200 K [12]. Lang and coworkers have shown that the isochronal recovery stage versus Debye temperatures within the III-V group is proportional to Θ_D^2 based on the previously reported data [12 and references therein].

The x-ray rocking curve technique [13] has been used to measure the damage and strains in ion implantation [5], in MeV ion irradiated garnet single crystals [14], and to analyze supperlattices [15]. In the next section, we show rocking curve data on various crystals bombarded with MeV ions.

EXPERIMENTAL RESULTS AND DISCUSSION

GaAs

Cr-compensation doped p-type semi-insulating GaAs (100) and Si- and Te-doped n-type GaAs (100), of resistivities of 1.4×10^{-3} and 8 10^{-3} Ohm-cm, respectively, were irradiated with Cl and O ions (3 to 15 MeV) to various doses (10^{13} to 5×10^{15} ions/cm^2) using the tandem accelerator at Caltech. The irradiation current density was typically 10^{11} to 10^{12} ions/cm^2 sec. The irradiation was done approximately normal to the sample surface which is about 2-3 degrees off the (100) plane. No channeling effect was observed. The irradiated samples were analyzed by the x-ray rocking curve technique described elsewhere [11] using a double-crystal x-ray diffractometer. The Bragg reflections of FeK 1 radiation from (400), (422), (511), and (333) planes have been recorded at each angle, which is typically changed in .001 degree steps.

The (400) rocking curves taken for a Cr-doped GaAs single crystal irradiated with a 15 MeV Cl ion beam (Range = $\sim$ 5.8um in GaAs) are given in Fig. 1 in order of increasing beam dose. The small single peak at zero angle is the diffraction signal from the undamaged substrate beyond the ion range. The diffraction pattern deviates toward negative angle from the substrate peak, varying with the ion beam dose, and corresponds to the strain development in

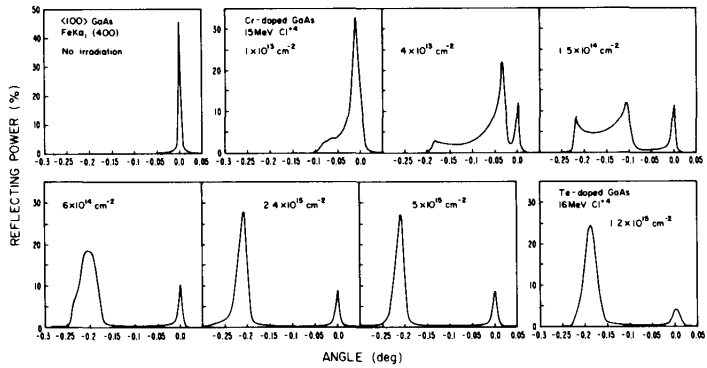

Fig. 1. (400) Bragg reflections for a Cr-doped GaAs (100) crystal are shown for increasing doses of 15 MeV Cl^{+4} ions. The peak at zero angle corresponds to the diffraction by the substrate crystal unaffected by the ion beam. The diffraction pattern deviates toward negative angle, and corresponds to the strain development in the surface layers by the ion irradiation. The single peak around .22 degrees after a high dose ($\geq 1.2 \times 10^{15}$ cm^{-2}) irradiation indicates a uniform lattice spacing like a single crystal in the suface layers.

the surface layers affected by the ion beam. After a high dose irradiation (e.g., $D \geq 1.2 \times 10^{15}$ ions/cm^2 for 15 MeV Cl) a single diffraction peak develops at a well defined angular separation from the substrate peak, with a small satellite of vanishing intensity for higher doses on the lower angle side, which means that the strain level in the surface layer saturates to a uniform lattice spacing like a single crystal, with a gradually amorphizing layer corresponding to the maximum nuclear energy loss region sandwiched between the surface crystal and substrate crystal. The strain perpendicular to the sample surface, in the surface layer can be calculated from the Bragg condition $n\lambda = 2d\sin\theta_B$ to be $\varepsilon^{\perp} = \Delta d/d = \Delta\theta_B \cot\theta_B$ for a symmetric reflection. Thus, the measured perpendicular strain, which is uniform after high dose irradiation, is $\sim 0.4\%$. The strain parallel to the sample surface (defined as "parallel strain" hereafter) can be measured by an asymmetric reflection. This strain saturation phenomenon from high dose irradiation is the same for other heavily doped GaAs crystals with approximately the same strain level (as shown in the last diagram in Fig. 1 for Te-doped GaAs). Cr-doped GaAs crystals were bombarded with Cl and O ions at different energies to clarify the strain production mechanism in the surface layers. The final strain level is the same for all the ions at different energies. The strain at the sample surface can be measured directly from the rocking curve data because the strain level at the surface is the lowest in the strain vs. depth distribution. The surface strain perpendicular to the surface is plotted versus increasing ion dose in Fig. 2a. The saturation dose is lower for ions with higher nuclear stopping power, for example, the saturation dose is $\sim 1.5 \times 10^{14}$/cm^2 for 3 MeV Cl and $\sim 1.2 \times 10^{15}$/cm^2 for 15 MeV Cl. Fig. 2b shows that at doses below the saturation dose the surface strain is proportional to the nuclear stopping power, S_n for a given ion, and is independent of the electronic stopping power, in contrast with the fact that MeV ions give rise to an enhanced sputtering yield from the surface of compound semiconductors [6].

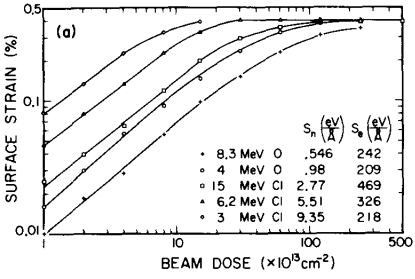

Fig. 2a. The perpendicular strain at the surface of GaAs (100) is given as a function of beam dose of various ions. The final "saturated" strain level is about the same for all the ion beams used. The higher the nuclear stopping power, the earlier the strain saturates.

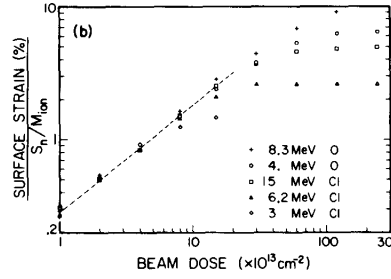

Fig.2 b. This plot was obtained by dividing the surface strain in (a) by S_n/M_{ion}. The data indicate that strain is proportional to $(S_n/M_{ion})D^{0.85}$.

To obtain the parallel strain in the surface layer, rocking curves were measured from asymmetric 422, 511, and 333 reflections for a Cr-doped GaAs (100) crystal bombarded with a 15 MeV Cl ion beam to a dose of $1.2 \times 10^{15}/cm^2$ and a 8.3 MeV O ion beam to $2.4 \times 10^{15}/cm^2$. The incident angle of the x-ray beam was $\theta_B - \phi$ with respect to the sample surface for the reflections measured, where ϕ is the reflecting plane angle with respect to the sample surface. For an asymmetric reflection, the angular separation of the strain peak from the substrate peak is related to the parallel and perpendicular strain by the following formula [15].

$$|\Delta\theta_B| = \varepsilon^{\perp}(\cos^2\phi\tan\theta_B \pm \sin\phi\cos\phi) + \varepsilon''(\sin^2\phi\tan\theta_B \mp \sin\phi\cos\phi) \qquad (1)$$

where the upper and lower signs refer to the incident angle of $\theta_B - \phi$ and $\theta_B + \phi$ with respect to the sample surface, respectively. Using Eq. (1) with the perpendicular strain found in the symmetric 400 reflection and the angular separation measured in the asymmetric rocking curves we find a parallel strain of essentially zero. This indicates a strong coupling of the strained surface layer to a much thicker substrate. The coupling does not permit the surface layer to expand laterally.

Fig. 3 shows the change of perpendicular strain level with temperature after 15 min. of isochronal annealing in vacuum for 15 MeV Cl doses of $1.2 \times 10^{15}/cm^2$. For the annealing, the GaAs sample was capped with another GaAs wafer to prevent As out-diffusion. There is an intensity jump of the reflecting power at a temperature 200° C < T < 300° C. This intensity jump is consistent with the 500 K recovery stage of electron irradiation-induced defects in GaAs [16]. Lang, Logan, and Kimmerling assigned the defects which recover at 500 K to Ga atom displacements [12] based on their work on the orientation dependence of defect production in GaAs. However, in more recent work, Pons and Borgoin reversed this assignment and proposed that it was due

to As atom displacements (from their work on orientation dependence of the introduction rates of electron traps E1, E2, and E3 as a function of electron irradiation energy) [17]. Pons and Bourgoin demonstrated that for electron energies below 0.6 MeV, there are more As-displacements than Ga-displacements, but above 0.6 MeV there are more Ga-displacements, consistent in trend (but not in magnitude) with the work of Lang, Logan, and Kimmerling. Since in the heavy MeV ion irradiation case the elastic process in the ion-solid collisions may correspond to higher energy electron irradiation, the 500 K recovery stage in MeV ion bombarded GaAs is more likely due to Ga-vacancies. But in contrast to the relatively well defined recovery stage of radiation induced vacancies, the strain level in the surface layers decreases rather smoothly in the temperature range 200° C to 500° C, approaching zero at 500° C. The absence of a sharp recovery stage of the strain indicates that the origin of uniform surface strain in GaAs is not due to vacancies alone. If the heavily damaged layer in the nuclear stopping region recrystallizes epitaxially upon annealing, then it will grow in direction both from the surface crystal layer and from the substrate crystal [1]. It can be seen that the surface crystal layer does not recover epitaxially to the original crystal from the fact that the reflecting power of the strain peak does not decrease by increasing the substrate reflecting power, but only the relative angular separation changes upon annealing.

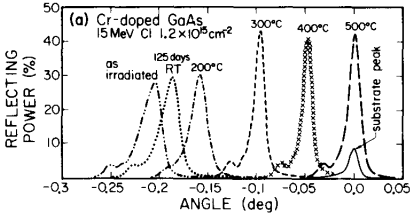

Fig. 3a. (400) Bragg reflection was taken for 15 MeV Cl ion bombarded GaAs (100) after a successive 15 min. isochronal annealing at the temperatures indicated. The broken curves represent the diffraction pattern from the surface strained layer. The solid curve at zero angle represents the diffraction pattern from the substrate, and is common for all the broken curves except the one taken after 500° C annealing. The broken curve 'as irradiated' is the rocking curve taken after ion irradiation, and the curve '125 days RT' after 125 days room temperature aging.

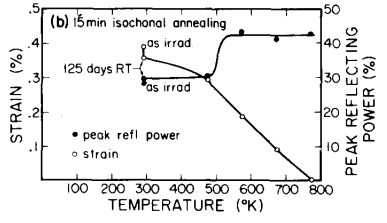

Fig. 3b. The perpendicular strain and the peak reflecting power of GaAs surface layer, obtained from (a), are given as a function of annealing temperature. The jump around 500 K in the peak reflecting power is consistent with the 500 K recovery stage of the radiation induced defects in GaAs. The strain decreases gradually with temperature.

The angular separation of the two peaks is not due to misorientation of the surface layer with respect to the substrate crystal as it did not change position after a 180 degree rotation of the sample about the surface normal.

The strain saturation in the surface layer indicates a saturation in the point defects responsible for the strain. There seem to be criteria for the strain saturation in room temperature MeV ion irradiation, i.e., (1) the point defects must be immobile near room temperature, (2) the electronic process in the energy loss of ion does not contribute to the damage production in the material, and (3) the energy loss into nuclear collisions is small enough so that no significant number of isolated disordered regions are created. If the point defects are mobile near or below room temperature as in Si

and Ge, then the surface strain does not appear. If the electronic process contributes to the damage production as in the track forming materials, then the high dose irradiation eventually converts the surface layer completely to the amorphous state. The above criteria are all satisfied in the MeV ion irradiation of GaAs. For a Cl ion in GaAs, for example, the electronic process is dominant in energy loss for ion energies greater than about 0.3 MeV [20]. The nuclear stopping power of a Cl ion in GaAs is about 36 eV/Å for 0.3 MeV, and less for higher energies (see Fig. 2a for higher energies), calculated from the Kr-C formula [21]. Assuming a threshold displacement energy of about 14 eV in the semiconductors [22], it can be seen that only isolated point defects will be created in the GaAs surface layer by the MeV ion irradiation. The saturation of disordered regions in keV ion implantation leads to a complete amorphous layer because the individual disordered regions overlap sufficiently [23]. The saturation of point defects in MeV ion irradiated GaAs, however, leads to a uniformly strained layer, i.e., a single crystal layer with a high uniform concentration of point defects. This point defect saturation phenomenon in GaAs can be considered in terms of the competition of the creation and the recovery processes of point defects, which are simultaneously going on during the irradiation. If the dense electronic ionization around the ion path plays any direct role in the recovery process, then the local final saturation level will be governed by the local ratio of the electronic stopping power to the nuclear stopping power. This does not seem to be the case because the ratio is the largest at the surface and decreases along the ion path in the present energy range. Fig. 2a also shows that the initial strain level is independent of the electronic stopping power. It is more likely that the recovery process is governed by the temperature in the material during the irradiation, which may be uniform along the ion path.

A detailed strain vs. depth distribution, which may be very useful in comparing the strain level with the nuclear stopping power, can be obtained by the analysis of the x-ray rocking curve data by a suitable x-ray diffraction theory. When the reflecting power of the surface strained layer does not exceed about 6% (as in 15 MeV Cl irradiation CaF_2), a kinematical diffraction theory can be used. When the reflecting power of the strained layer is larger than about 6%, a dynamic theory must be used. We are currently developing a capability to analyse the rocking curves using the dynamic theory.

Si and CaF_2

A 15 MeV Cl ion beam was used to irradiate n-type Si (111) of resistivity .005-.02 cm and CaF_2 (111) single crystals to various doses. In Fig. 4 the rocking curve data for Si show that the strain level in Si is generally very low and that the maximum strain reached in the maximum nuclear stopping layer is around 0.06% before that layer becomes amorphous at a dose of $1.25 \times 10^{14}/cm^2$. The data also show that no appreciable strain is induced in the surface layer except for a very low strain of about 0.02%, which may be from the layers adjacent to the maximum nuclear stopping layer. The zero strain in the surface layer can be ascribed to the fact that the point defects in Si, vacancies and interstitials, are mobile at room temperature [12] and that the elemental semiconductors do not have antisite defects, unlike the compound semiconductors. The antisite defects generally have a higher annealing temperature than vacancies. The strain in the higher nuclear stopping region around the region of maximum nuclear stopping power can be from the defect complexes in Si. Isolated amorphous regions can also contribute to the strain measured by x-rays by the strain field around the isolated disordered region. The influence of this effect on the measured total strain has not been analysed.

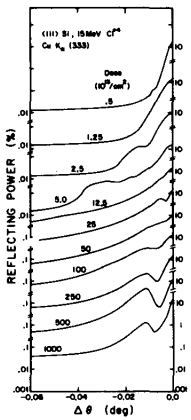

Fig. 4. (333) Bragg reflection from Si <111> bombarded by a 15 MeV Cl ion beam is shown. The substrate peak is at zero angle. The angular deviation of the diffraction pattern is small compared with GaAs or CaF_2. The strain giving rise to the diffraction pattern is in and around the region of maximum nuclear stopping power.

The rocking curves taken for a CaF_2 (111) single crystal are shown as a function of beam dose in Fig. 5a. When the maximum reflecting power of the strained layer is less than $\sim 6\%$, the strain and damage depth profile can be obtained by a kinematical x-ray diffraction theory analysis of the rocking curve data [11,13]. The strain/damage depth distribution (Fig. 5b) obtained by this analysis shows that the nuclear collision process, which is the dominant energy loss process near the end of ion range, is effective in producing strain and damage. The nearly constant strain level toward the surface is consistent with the fact that the nuclear stopping power in the high ion-velocity region $v \leq e^2/\hbar$ is nearly constant [18] and that the radial dimension of the nuclear damage track in an insulator is proportional to $(dE/dx)^{1/3}$ [19]. The radiation induced defects which are responsible for the strain production have not been determined.

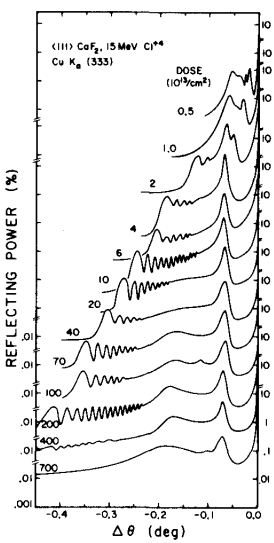

Fig. 5a. (333) Bragg reflection from a 15 MeV Cl bombarded CaF_2 <111> single crystal. The substrate peak is at zero angle.

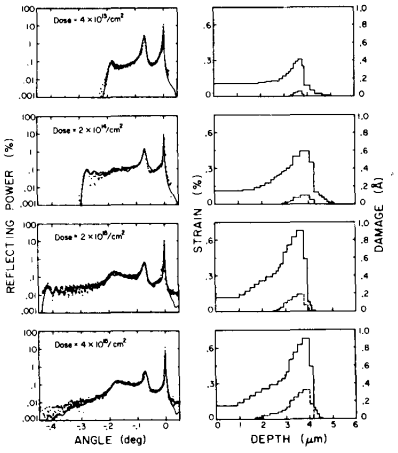

Fig. 5b. The dots are the experimental reflecting power and the solid curves are the calculated reflecting power using a kinematical x-ray diffraction theory, assuming the strain/damage depth distribution given on the right-hand side. The damage is defined by the mean atomic displacement (Å) from the lattice site, which appears in a Debye-Weller factor in the structure factor.

CONCLUSION

A high dose irradiaton of semi-insulating and highly doped GaAs (100) single crystals with MeV ions has been shown to produce a uniformly strained single layer in the surface region. The strain saturation in GaAs seems to be due to the point defect saturation in the surface layer. In the early stage of irradiation (i.e., at low dose), the strain produced at the surface is proportional to the nuclear stopping power for a given ion beam. The surface strain saturates at the same level (i.e., $\sim 0.4\%$ for the perpendicular strain) regardless of the ion beam used and the beam energy. The annealing behavior shows that there is a recovery stage of radiation induced vacancies at 200° C $< T \leq 300^{\circ}$ C in the surface single crystal layer and the strain is not due to vacancies alone and that, unlike the rather well defined recovery stages of the radiation-induced specific defects, the strain decreases gradually with temperature. The strain goes to zero at $T \leq 500^{\circ}$ C recovering the original lattice spacing. This annealing behavior of the strain indicates that the point defects in GaAs, i.e., vacancies, interstitials and antisite defects (the recovery stage of the antisite defect, As_{Ga}, is around 500° C [24]), are responsible for the strain in the surface layer. An EPR measurement of MeV ion beam induced antisite defects in GaAs, and some independent measurement of specific point defects as a function of beam dose in relation to the rocking curve measurement of lattice strain may be important in determining the importance of each point defect type in producing the strain.

MeV ion induced strain in Si is generally very low with no appreciable strain in the surface layer, consistent with the fact that no electronic ionization-induced enhanced erosion exists in the MeV ion irradiated Si. The strain induced in an insulating single crystal CaF_2 has been measured with the x-ray rocking curve technique, and quantitative strain and damage depth distributions were obtained by a kinematical diffraction theory analysis.

ACKNOWLEDGEMENTS

This work was supported in part by the National Science Foundation [DMR83-18274] and the Caltech President's Fund.

REFERENCES

1. D. K. Sadana, H. Choski, J. Washburn, and N. W. Cheung, Appl. Phys. Lett. 44, 301 (1984).
2. V. S. Speriosu, B. M. Paine, M-A. Nicolet, and H. L. Glass, Appl. Phys. Lett. 40, 604 (1982).
3. J. S. Harris, F. H. Eisen, B. Welch, J. D. Haskell, R. D. Pashly, and J. W. Mayer, Appl. Phys. Lett. 21, 601 (1972).
4. R. T. Hodgson, J. E. E. Baglin, R. Pal, J. M. Neri, and D. A. Hammer, Appl. Phys. Lett. 37, 187 (1980).
5. R. L. Fleischer, P. B. Price, and R. M. Walker, Nuclear Tracks in Solids, (Univ. of California Press, Berkeley, 1975).
6. Y. Qiu, J. E. Griffith, and T. A. Tombrello, Nucl. Instr. Meth. B1, 118 (1984); T. A. Tombrello, Int. J. Mass Spec. Ion Phys. 53, 307 (1983).
7. Y. Qiu, J. E. Griffith, W. J. Meng, and T. A. Tombrello, Rad. Eff. 70, 231 (1983).
8. T. A. Tombrello, Nucl. Instr. Meth, B2, 555 (1984); T. A. Tombrello, C. R. Wie, N. Itoh, and T. Nakyama, Phys. Lett. 100A, 42 (1984); T. A. Tombrello, Nucl. Instr. Meth. B1, 23 (1984).
9. T. A. Tombrello, Nucl. Instr. Meth 218, 679 (1983); T. A. Tombrello, J. Phys. Soc. Jap. in press (1984).
10. M. H. Mendenhall, Ph.D. Thesis, California Institute of Technology (1983); T. A. Tombrello, J. Mat. Sci. Eng., in press (1984); C. R. Wie, C. R. Shi, M. H. Mendenhall, R. P. Livi, T. Vreeland, Jr., and T. A. Tombrello, Nucl. Instr. Meth., in press (1984); S. Paine, C. R. Wie, M. H. Mendenhall, R. P. Livi, T. Vreeland, Jr., and T. A. Tombrello, Mat. Res. Soc. Symp. Proc., submitted (1984).
11. C. R. Wie, T. Vreeland, Jr., and T. A. Tombrello, Nucl. Instr. Meth., submitted (1984).
12. D. V. Lang, R. A. Logan, and L. C. Kimmerling, Phys. Rev. B 15, 4874 (1977).
13. V. S. Speriosu, J. Appl. Phys. 52, 6094 (1981); G. L. Miller, R. A. Boie, P. L. Cowan, J. A. Golvchenko, R. W. Kerr, and D. A. H. Robinson, Rev. Sci. Instr. 50, 1062 (1979).
14. B. Strocka, G. Bartels, and R. Spohr, Appl. Phys. 21, 141 (1980).
15. V. S. Speriosu and T. Vreeland, Jr., J. Appl. Phys. 56, 1591 (1984).
16. K. Thommen, Rad. Eff. 2, 201 (1970).
17. D. Pons and J. Borgoin, Phys. Rev. Lett. 47, 1293 (1981).
18. J. Lindhard and M. Scharff, Phys. Rev. 124, 128 (1961).
19. T. A. Tombrello, Nucl. Instr. Meth. B1, 23 (1984).
20. J. W. Mayer, L. Erikson, and J. A. Davis, Ion Implantation in Semiconductors (Academic Press, New York and London, 1970, p. 23).
21. W. D. Wilson, L. G. Haggmark, and J. P. Biersack, Phys. Rev. B 15, 2458 (1977).
22. A. Sosin and W. Bauer, Studies in Radiation Effects, ed. G. J. Dienes, Vol. 3 (Gordon and Breach, New York, 1969).
23. J. W. Mayer, L. Erikson, and J. A. Davis, Ion Implantation in Semiconductors (Academic Press, New York and London, 1970, p. 99).
24. R. Wörner, U. Kaufman, and J. Schneider, Appl. Phys. Lett. 40, 141 (1982).